



HAL
open science

Degradation of sulfapyridine antibiotics by chlorination in a pilot-scale water distribution system: kinetics, THMs, and DFT studies

Jie Ji, Changjie Shi, Luo Xu, Kai Zhang, Yunshu Zhang, Cong Li, Eric Lichtfouse

► To cite this version:

Jie Ji, Changjie Shi, Luo Xu, Kai Zhang, Yunshu Zhang, et al.. Degradation of sulfapyridine antibiotics by chlorination in a pilot-scale water distribution system: kinetics, THMs, and DFT studies. *Environmental Science: Water Research and Technology*, 2022, 10.1039/d2ew00198e . hal-03788823

HAL Id: hal-03788823

<https://hal.science/hal-03788823>

Submitted on 27 Sep 2022

HAL is a multi-disciplinary open access archive for the deposit and dissemination of scientific research documents, whether they are published or not. The documents may come from teaching and research institutions in France or abroad, or from public or private research centers.

L'archive ouverte pluridisciplinaire **HAL**, est destinée au dépôt et à la diffusion de documents scientifiques de niveau recherche, publiés ou non, émanant des établissements d'enseignement et de recherche français ou étrangers, des laboratoires publics ou privés.

Degradation of sulfapyridine antibiotics by chlorination in a pilot-scale water distribution system: kinetics, THMs, and DFT studies†

Jie Ji,^a Changjie Shi,^a Luo Xu,^a Kai Zhang,^a YunShu Zhang,^a
Cong Li ^{*a} and Eric Lichtfouse^b

Sulfonamides (SAs) have been proved to damage organisms if the contact time last over the long term. Therefore, sulfapyridine (SPD), as typical one, was chosen as a target to be investigated. For the study, the degradation kinetic of SPD in the chlorination stage of a pilot-scale water distribution system (WDS) was studied. The result showed that the degradation of SPD simultaneously followed the first-order and pseudo second-order kinetic model. In the beakers tests or WDS, the reaction rate reaches maximum value when the pH is about 7. The degradation rate of SPD would be higher with the increase of water velocity in the WDS. Different pipe materials were studied and the degradation effect of SPD was in the following order: stainless-steel pipe > ductile iron pipe > polyethylene (PE) pipe. There was a significant increase in the content of trihalomethanes (THMs) when chlorination of tap water containing SPD in both the WDS and the beakers system were performed. The mechanism of this process was analyzed in combination with the intermediate products degraded by SPD in the process. In addition, density functional theory (DFT) calculations were performed to assist in the identification of 6 intermediates and possible degradation pathways.

Water impact

For the study, the degradation kinetic of sulfapyridine in the chlorination stage of a pilot-scale water distribution system was studied. The result showed that the degradation of sulfapyridine simultaneously followed the pseudo first-order and second-order kinetic model. The effect of three types of pipes on the degradation of sulfapyridine was compared, the degradation effect of sulfapyridine was in the following order: stainless-steel pipe > ductile iron pipe > polyethylene pipe. Detection of intermediate products of sulfapyridine degradation combined with DFT analysis to infer the possible degradation pathways of sulfapyridine. In addition, the generation of disinfection by-products after chlorination treatment was explored. This experiment provides a reference for the chlorination treatment of sulfonamide antibiotics in actual pipe network water.

1 Introduction

Much attention has been paid to the occurrence of antibiotics in the environment in the past decade.¹ SAs refer to one type of synthetic antimicrobial agents that contain the sulfonamide group, including sulfamethoxazole, sulfacetamide, sulfadiazine, sulfadoxine, sulfasalazine, sulfamethizole, sulfisoxazole and sulfanilamide and so on.² SAs, as effective antibiotics, have been frequently produced and consumed all around the world. Therefore, they are one of the typical pollutants in surface water, soils, and

wastewater.^{3–5} Klein *et al.* reported that the antibiotic consumed globally reached 34.8 billion in 2015.⁶ There are more than 20 000 tons of SAs brought into the environment every year.⁷ Sulfonamide residues result in the spread of antibiotic resistance genes with potential toxicity. SPD, as one of the commonly used sulfonamide antibiotic, has been widely applied as veterinary drugs and repeatedly detected in aquatic environment.⁸ Many research results showed diverse negative effects of SPD such as bio-toxicity and endocrine disruption for both aquatic wildlife and mankind.⁹ Therefore, it is necessary to establish an efficient chemical oxidation process to remove SPD.

Recently, many researchers have concentrated on photocatalytic degradation of SPD.^{10–12} However, the HOCl/OCl-chlorination is currently the most popular disinfection method due to its strong oxidizing ability and long-lasting effect.¹³ There are many hazardous intermediates and

^a School of Environment and Architecture, University of Shanghai for Science and Technology, Shanghai 200093, China. E-mail: congil@aliyun.com

^b CNRS, IRD, INRA, Coll France, CEREGE, Aix-Marseille Univ, 13100 Aix en Provence, France

† Electronic supplementary information (ESI) available. See DOI: <https://doi.org/10.1039/d2ew00198e>

carcinogenic halogenated disinfection by-products (DBPs) produced during chlorination.¹⁴ The report showed that approximately 70% SPD was degraded about 60 min in the UV/chlorine process (pH = 5).¹⁵ In addition, He *et al.* studied the degradation of SPD in the Cu_{0.76}Co_{2.24}O₄/SBA-15/PMS (CCSP) process and the SPD could be utterly degraded after 90 min under the suitable reaction condition.⁸ Most previous studies on the degradation of SPD were taken in beakers tests. However, there are few studies on the degradation of SPD by chlorination in WDS.

The surplus micro-pollutants like SPD may react with the free chlorine in the WDS, generating by-products that threaten human health.¹⁶ Therefore, it is essential to study the DBPs of SPD in the WDS. Our research group has made efforts to investigate the elimination of pollutants in the WDS which contain the degradation kinetic, formation of intermediate products and final DBPs. Dong *et al.* investigated the kinetics and pathway of estriol chlorination in the WDS¹⁷ and that of sulfadiazine chlorination in the WDS.¹⁸ Nevertheless, intermediate products analysis and degradation pathways of SPD in the WDS has not been studied so far.

The main objectives of this study were to investigate the degradation process of SPD by chlorination in the WDS: (1) investigate the kinetic of SPD degradation by chlorination; (2) study the formation of THMs produced during SPD chlorination; (3) deduce the probable degradation pathway of SPD with the calculation result of DFT.

2 Materials and methods

2.1 Chemicals and reagents

Sulfapyridine (SPD, C₁₀H₁₀N₄O₂S, AR ≥95%) was purchased from Aladdin (Shanghai, China). The physicochemical properties of SPD were summarized in Table S1.† Sodium hypochlorite (NaClO, available chlorine 10%) was purchased from Aladdin (Shanghai, China). Sodium dihydrogen phosphate (NaH₂PO₄, AR grade), sodium thiosulfate (Na₂S₂O₃, CP grade), sodium hydroxide (NaOH, AR grade), disodium hydrogen phosphate (Na₂HPO₄, AR grade), and ammonium acetate (CH₃COONH₄, AR grade) were purchased from Sinopharm Chemical Reagent (Shanghai, China). Methyl *tert*-butyl ether (MTBE), dichloromethane, methanol, phosphoric acid, acetonitrile, and *N*-hexane were obtained from Thermo Fisher (Shanghai, China) with chromatography grade. The pure water was obtained from a Milli-Q system.

2.2 Experimental procedures

SPD degradation experiments were performed both in beakers and WDS. Three separate loops made of ductile iron (loop A), PE (loop B), and stainless-steel (loop C) respectively, were used in the pilot scale WDS in Fig. S1.† With the popularity of ductile iron pipes in the world, ductile iron pipes were used as the main pipe material in this paper.

The original dosage of SPD was set at 200 µg L⁻¹ in the WDS experiments. We set the basic experimental conditions

as free chlorine 0.8 mg L⁻¹, temperature 25 °C, flow rate 1.0 m s⁻¹ and pH 7 ± 0.2. Different experimental conditions were set as pH (6.6, 7.0, 7.4, 7.8, and 8.2), flow velocities (0.7, 1.0, 1.3, and 1.5 m s⁻¹) and pipe materials (ductile iron, PE, and stainless-steel). After reaction, 10 mL samples were taken at pre-designed time interval. Based on previous article,¹⁹ the samples should be quickly quenched in excess Na₂S₂O₃ solution. The beakers tests were carried out in a brown glass bottle under dark conditions and the samples were taken at the same sampling time of the WDS. Before sampling, 0.2 mL sodium thiosulfate (0.2 mol L⁻¹) solution should be added into the sample bottle as the reaction quenching agent.

2.3 Analytical procedures

The concentration of SPD was analyzed by a high-performance liquid chromatography (HPLC) (Essentia LC15C, Shimadzu, Japan) equipped with an ultraviolet detector (G1314B, Agilent, Santa Clara, CA, USA). A Eclipse XDB-C18 column (4.6 mm × 150 mm, 5 µm) was used in the investigation at 30 °C. Acetonitrile and 1% phosphoric acid solution with the ratio of 95:5 (v/v) was the mobile phase at a flow of 1.0 mL min⁻¹.¹¹

Solid phase extraction (SPE) was used to pretreat for the analysis of degradation intermediates. The solid phase was firstly activated by 15 mL methanol, then 15 mL pure water. 300 mL samples were then loaded through cartridges (Oasis HLB) at 1–2 mL min⁻¹. The final samples were eluted by 5 mL dichloromethane and 5 mL MTBE respectively and concentrated to 1.0 mL through nitrogen purge. The degradation intermediates of SPD were detected by LC-MS (Agilent 6460) equipped with an Eclipse XDB-C18 column (4.6 mm × 150 mm, 5 µm). A positive electrospray ionization mode (ESI⁺) was applied in the analysis. The working conditions of the column were as following: the wavelength was 253 nm, the mobile phase was a mixture of water and acetonitrile at a ratio of 80:20 (v/v), the flow rate was 0.3 mL min⁻¹ and the column temperature was 30 °C. Other important operating conditions were as following: the carrier gas temperature was 325 °C, the carrier gas flow rate was 5 L min⁻¹, the sprayer pressure was 45 psi, the protective gas temperature was 345 °C, the flow rate was 11 L min⁻¹, the capillary voltage was 3000 V (+)/3500 V (-), the nozzle voltage was 0 V (+)/500 V (-), and the cracking voltage was 135 V.

THMs were detected by a gas chromatography with an electron capture detector (GC-ECD) (GC-450, Varian, Palo Alto, CA, USA) equipped with injection system for purge and trap pretreatment in Table S2.† (Teledyne TekmarTM, Atomx). The GC column was a DB-5 capillary column (30 m × 0.25 mm, 0.25 µm). The initial temperature of the oven was 60 °C, holding for 10 min and then increasing by 20 °C to 250 °C every minute. The temperatures of the injection port and detector were 150 °C and 300 °C, respectively.²⁰ Chromatogram and standard curves of THMs were provided in Fig. S2 and Table S3.†

2.4 Computational modeling

All quantum chemical calculations presented in this paper were carried out using Gaussian09 (G09) program.²¹ Firstly, the hybrid B3LYP/6-31+G (d,p) was used to optimize the structure of SPD in water. Then, the HOMO orbital and NBO atomic charge distribution of SPD were calculated by using the natural bond orbital theory (NBO) method with the key words of pop = (npa, reg). The high value of the HOMO was the most possible place for electrophilic reactions.²²

3 Results and discussion

3.1 Degradation kinetics of SPD by chlorination

This section mainly studied the influence of residual chlorine concentration on the degradation rate of SPD. Fig. 1a and c showed the degradation curves of SPD in the WDS and beakers tests under different chlorine concentrations respectively. In Fig. 1a, when the residual chlorine concentration was 0.8 mg L⁻¹, more than 99% of SPD could be degraded at the beginning 30 minutes of the reaction, and the increase of residual chlorine concentration in the WDS had a remarkable promoting effect on the degradation of SPD. The first-order kinetic equation shown in eqn (1) was used to fit the degradation curves.

$$r = \frac{d[\text{SPD}]_t}{dt} = k_1[\text{SPD}]_t \quad (1)$$

In the eqn (1), r is the reaction rate, $[\text{SPD}]_t$ is the concentration of SPD at time t , k_1 is the first order reaction rate constant. Eqn (1) can be transformed into eqn (2):

$$\ln\left(\frac{[\text{SPD}]_t}{[\text{SPD}]_0}\right) = -k_1t + b \quad (2)$$

b is a constant in the eqn (2).

Fig. 1b and d showed the results of the data fitted of the degradation curves. The linear correlation coefficient R^2 and the first order kinetic constant k_1 were shown in Table S4.† When the residual chlorine concentrations were 0.6, 0.8, 1.0 and 1.2 mg L⁻¹, the linear correlation coefficients R^2 were 0.994, 0.985, 0.978 and 0.962 in the WDS and when the residual chlorine concentrations were 0.2, 0.4, 0.6, 0.8, 1.0 and 1.2 mg L⁻¹, R^2 were 0.967, 0.997, 0.998, 0.998, 0.997 and 0.995 in the beakers tests respectively, showing a good correlation. Therefore, the reaction of free active chlorine (FAC) with SPD in beakers tests is considered to be in accordance with the first-order kinetic model. The study found that the correlation coefficients of the beakers tests were generally higher than that of the WDS. This may be due to the influence of TOC and pipe wall in the WDS, but there was still a good correlation (all >0.96 in WDS). Therefore, the reaction between FAC and SPD in the WDS and beakers tests basically fit to the first-order kinetic model (eqn (1)).

Some papers pointed out that the reaction of some organic compounds with chlorine was a second order reaction,²³ and it was also investigated in this study. If the reaction of FAC and SPD fits to the second order kinetic model, then:

$$r = \frac{d[\text{SPD}]_t}{dt} = k_2[\text{FAC}]_t[\text{SPD}]_t \quad (3)$$

In the eqn (3), k_2 is the second-order reaction rate constant, $[\text{FAC}]_t$ is the chlorine concentration at time t . Because the molar concentration of residual chlorine was more than 10 times that of the target, the change of FAC during the reaction was negligible. Fig. S3.† showed the linear correlation coefficient $R^2 = 0.96$ in the WDS and $R^2 = 0.97$ in the beakers tests which can verify that k_1 has a proportional relationship with $[\text{FAC}]$. Therefore, the SPD reaction fits to the second-order reaction kinetic model. Table S5.† showed the second-order kinetic constants in WDS is also lower than that in beakers tests. The reason can be explained as following: compared with beakers tests, soluble organic matter in WDS would consume part of FAC, which would decrease the concentration of it. According to $k_1 = k_2[\text{FAC}] + b$, the immediate reaction rate in WDS also decreases with the reaction process, so the overall k_1 decreases, which then leads to the actual k_2 of the pipe network also become lower compared to the beakers tests.

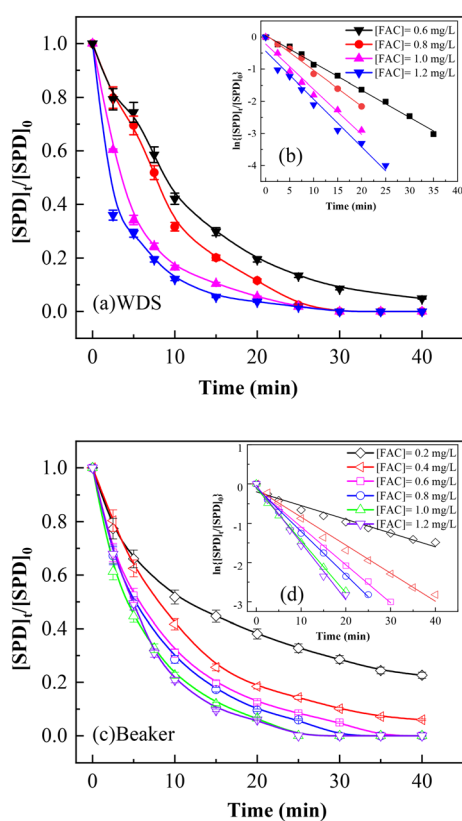


Fig. 1 Degradation of SPD at different chlorine concentrations. (a) WDS. (b) First-order kinetic fitting in WDS. (c) Beakers. (d) First-order kinetic fitting in beakers.

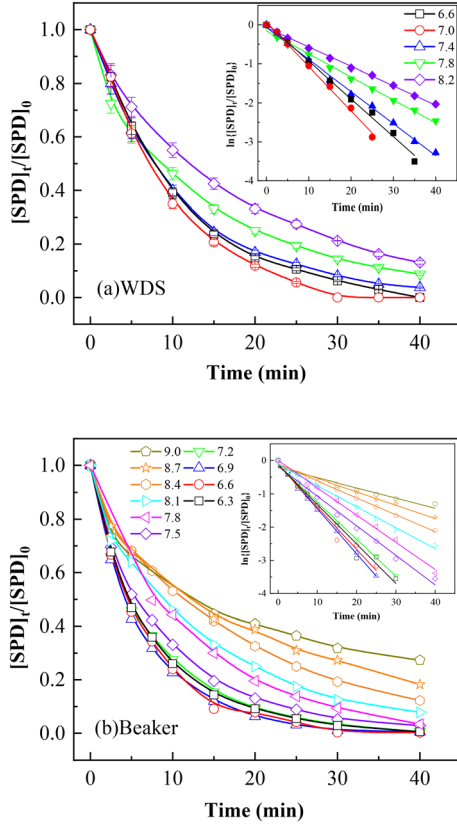


Fig. 2 Effect of initial pH on the degradation of SPD. (a) WDS. (b) Beaker.

3.2 Effects of SPD degradation by chlorination

3.2.1 pH. In order to compare the reaction rates under different pH conditions, the first-order kinetic model was applied to fit the reaction process under different pH conditions. Fig. 2 showed the reaction rate constant reach the maximum values at the pH of about 7 in both the beakers tests and WDS.

Text S2† showed the dissociation reaction of FAC and SPD. Due to dissociation reaction, residual chlorine generally has two forms as ClO^- and HClO which is chemically active and easily decomposes into HCl and O_2 in aqueous solutions (eqn (4) and S2†). SPD has three forms as SPD^+ , SPD and SPD^- (eqn (5) and S7 and S8†).

$$[\text{FAC}] = [\text{HClO}] + [\text{ClO}^-] = \sum_{i=1}^2 \alpha_i [\text{FAC}] \quad (4)$$

$$[\text{SPD}]_{\text{tot}} = [\text{SPD}^+] + [\text{SPD}] + [\text{SPD}^-] = \sum_{j=1}^3 \beta_j [\text{SPD}]_{\text{tot}} \quad (5)$$

According to Fig. S4† the FAC primarily exists in the form of HClO under acid to neutral conditions and ClO^- under alkaline conditions. The standard electrode potential of HClO/Cl^- pair and ClO^-/Cl^- pair is 1.482 and 0.89

respectively, so the oxidation of HClO with the same concentration is stronger than that of ClO^- .²⁴ The results showed that SPD degraded faster under neutral condition. According to Nernst eqn (6) and (7), the higher the pH is, the lower the $[\text{H}^+]$ is. Moreover, the lower the electrode potential of the two pairs is, the lower the oxidation is.²⁵

$$E(\text{HClO}/\text{Cl}^-) = E^0 + \frac{0.0592}{2} \lg \frac{[\text{Oxidation state}][\text{H}^+]}{[\text{Reduced state}]} \quad (6)$$

$$E(\text{ClO}^-/\text{Cl}^-) = E^0 + \frac{0.0592}{2} \lg \frac{[\text{Oxidation state}]}{[\text{Reduced state}][\text{OH}^-]} \quad (7)$$

In order to further quantify the influence of pH, this study proposed an orthogonal reaction function model based on the dissociation of SPD and FAC, revealing the relationship between the second-order kinetic constant and pH ($[\text{H}^+]$). Eqn (8) and S14 and S15† were the relationship between the total reaction and the orthogonal reaction of each component.

$$\frac{d[\text{SPD}]_{\text{tot}}}{dt} = -k_2[\text{FAC}][\text{SPD}] = -\sum_{i=1}^2 \sum_{j=1}^3 k_{ij} \alpha_i [\text{FAC}] \beta_j [\text{SPD}] \quad (8)$$

k_{ij} is the second-order kinetic constant of the orthogonal reaction between the two dissociation forms of FAC and the three dissociation forms of SPD. Fig. S5† showed the fitting results of k_2 -pH of SPD chlorination process in the WDS and beakers tests. According to the $R^2 = 0.987$, the model had a good correlation with the reaction of SPD chlorination in the WDS and beakers tests. Therefore, the model can predict the rate of SPD chlorination when the pH changes.

3.2.2 Velocity. Fig. 3 showed the k_1 of chlorinated SPD increased from $4.34 \times 10^{-2} \text{ min}^{-1}$ to $12.18 \times 10^{-2} \text{ min}^{-1}$ in the flow rate range of 0.7–1.0 m s^{-1} and the degradation rate increased obviously with the increase of flow rate. When the flow rate changed from 1.0 m s^{-1} to 1.5 m s^{-1} , the first-order kinetic constants were 12.18×10^{-2} , 13.97×10^{-2} and $13.15 \times 10^{-2} \text{ min}^{-1}$ respectively. Thus, the change of SPD degradation rate with the increase of flow rate was not obvious in the flow rate range from 1.0 to 1.5 m s^{-1} .

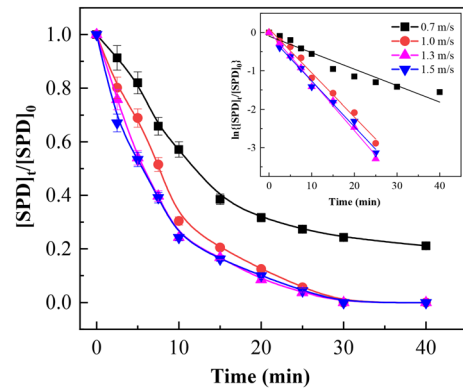


Fig. 3 Degradation of SPD at different flow velocity.

Generally, the reaction rate in liquid phase will be affected by mass transferring. In turbulent flow, the mass transferring rate will increase with the increase of Reynolds number ($Re = \frac{\rho v d}{\mu}$, where ρ is the fluid density, v is the flow velocity, d is the pipe diameter, and μ is the viscosity). The higher the mass transferring rate is, the faster the mixing of substances and molecules in liquid phase is and the faster the reaction rate is.^{26,27} After calculation, when the flow velocity in the pipe is 0.7, 1.0, 1.3 and 1.5 m s⁻¹, the Re are 103 600, 148 000, 177 600 and 222 000 respectively, and all Re >2300, which proves that it is a turbulent state in the pipe. Therefore, when the flow velocity increases from 0.7 to 1.0 m s⁻¹, the value of k_1 increases significantly; when the flow velocity >1.0 m s⁻¹, the change of k_1 value is not obvious, and 1.5 m s⁻¹ is equivalent to 1.0 m s⁻¹ and 1.3 m s⁻¹, because the mass transfer effect reaches the limit when the flow velocity >1.0 m s⁻¹ (*i.e.* Re >177 600).

3.2.3 Pipe materials. In order to investigate the effect of different pipe materials on the chlorinated degradation of SPD, PE pipe, stainless steel pipe and ductile iron pipe were selected to investigate the chlorinated degradation respectively. In Fig. 4, the degradation capability of SPD chlorination was followed by stainless-steel pipe, ductile iron pipe and PE pipe. The reason was that under the influence of turbulence, the pipe scale on the pipe wall fell off and mixed with the tap water in the WDS. The level of soluble iron was different in the WDS of different materials. The iron ion concentration of stainless-steel pipe was the highest (0.78 mg L⁻¹) and the iron ion concentration of ductile iron pipe was (0.12 mg L⁻¹) due to the lining of cement. Because soluble iron can promote the reaction,²⁸ the chlorination degradation efficiency of SPD in stainless-steel pipe was higher than that in ductile iron pipe and PE pipe.

3.3 The formation of THMs

Trihalomethanes (THMs) are the most typical DBPs in waters. The DBPs of THMs in the chlorination process of SPD were monitored. Some researchers reported that in the disinfection process of water containing PPCPs, the number

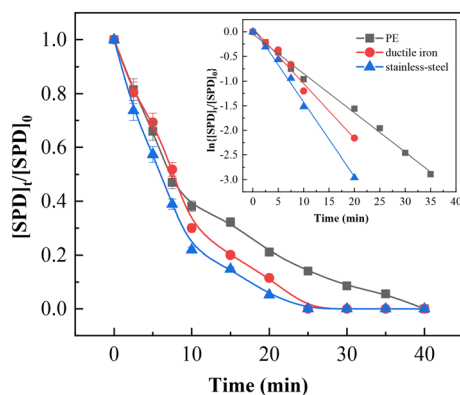


Fig. 4 Degradation of SPD in different pipe materials.

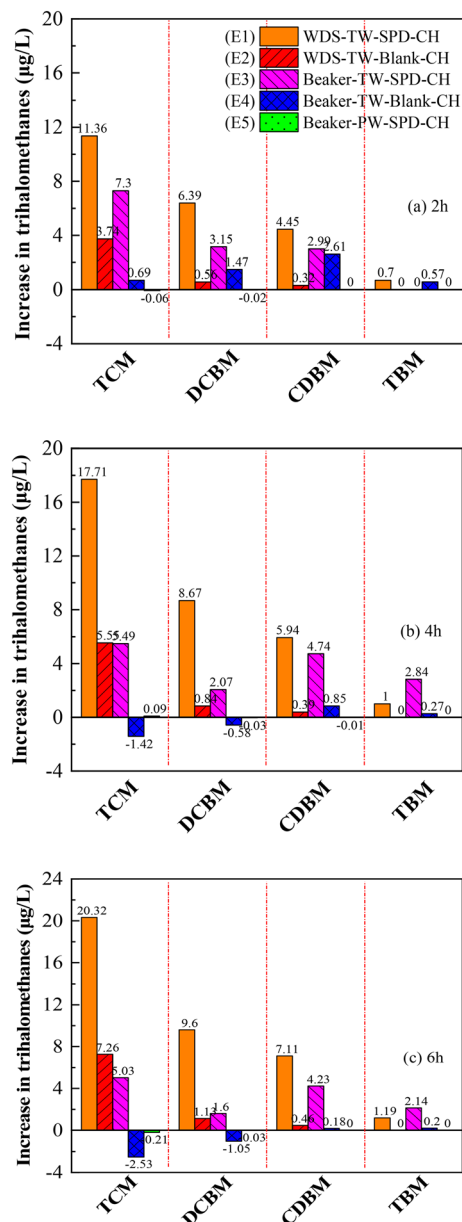


Fig. 5 The increase of THMs at 2 h (a), 4 h (b) and 6 h (c).

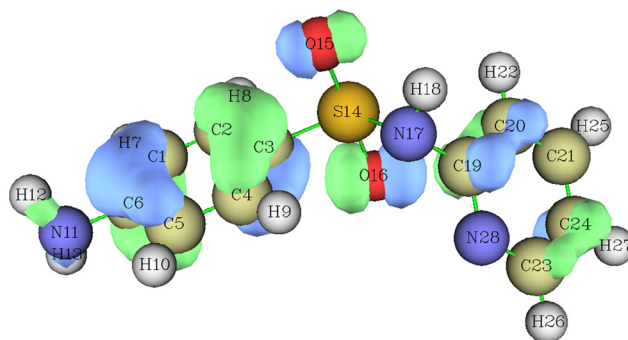


Fig. 6 Structure optimized SPD molecule and its Homo orbital analysis.

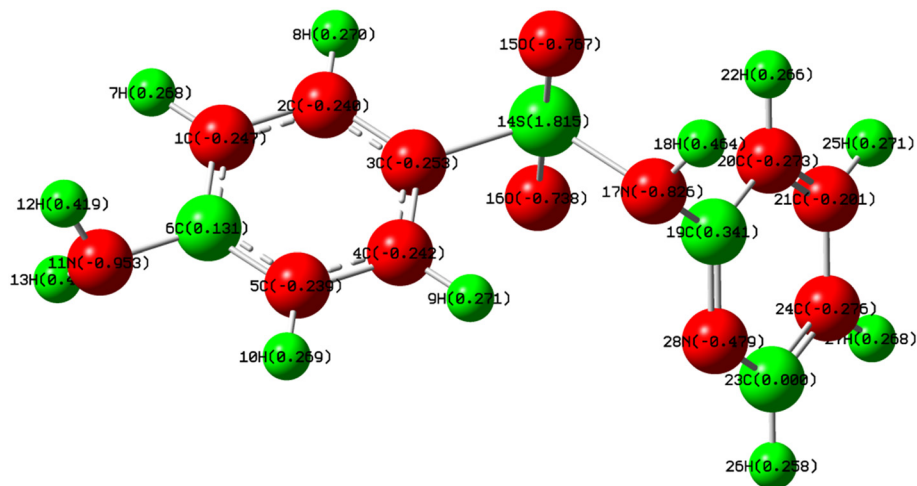


Fig. 7 NBO atomic charge distribution of SPD molecule.

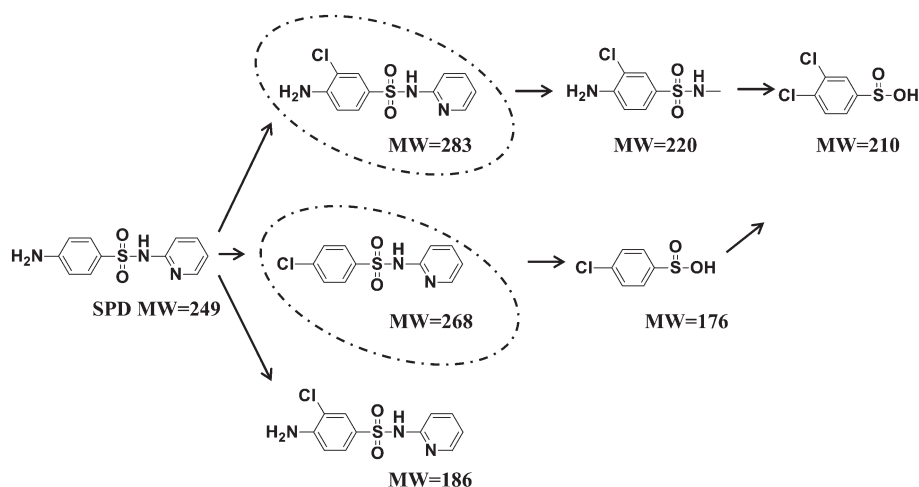


Fig. 8 Reaction path of SPD chlorination.

of THMs and haloacetic acid-like DBPs will increase.^{29,30} Ding *et al.*³¹ discovered that the contact reaction of paracetamol with chlorine in pure water for 12 h will produce trichloromethane and HAAs with the same molar concentration as paracetamol. Dong *et al.*³² also found that the amount of THMs produced by chlorine disinfection increased in the tap water containing sulfamethazine in the WDS compared to the tap water without sulfamethazine. For the sake of investigating the causes of THMs, five groups of experiments (E1–E5) were set up for comparison.

Fig. 5a showed the increasing order of THMs in the WDS was trichloromethane > dichloromonobromomethane > monochlorodibromomethane > tribromomethane at 2 h. The amount of THMs produced by SPD chlorination in the WDS was more than that without SPD. However, the increase of THMs produced by chlorination of same concentration SPD in pure water was almost zero in E5. This showed the amount of THMs produced by chlorination of SPD itself was very low, but it had a significant promoting effect on THMs generation in the WDS. The tap water was taken out from the WDS and

the SPD chlorination experiments were carried out in the beakers (E3). The increase of THMs was also higher than that in E2 and E4, but lower than that in E1, which indicated that the organic matter in the tap water was affected by SPD and produced more DBPs. In addition, the organic compounds attached to the pipe wall were released due to the effect of SPD and react with FAC to produce THMs.

As shown in Fig. 5b and c, the amount of THMs in the WDS increased further due to the cumulative effect from 4 h to 6 h. When the WDS contains SPD, the total increase of THMs is $38.22 \mu\text{g L}^{-1}$ at 6 h, while without SPD, the total increase of THMs is only $8.85 \mu\text{g L}^{-1}$ at 6 h.

3.4 Possible degradation pathway and DFT calculation

The above results showed that SPD itself did not generate THMs under chlorination. It will be converted into other products under the chlorination. For the study, the HOMO orbital and NBO atomic charge distribution of SPD molecule were calculated by density functional theory (DFT), which

was combined with LC-MS analysis method to speculate the possible degradation pathways.^{21,33} Fig. S6† showed the total ion chromatogram (TIC) of SPD during chlorination and four intermediates were analyzed. As shown in Fig. S7 and Table S6,† the chlorination products of SPD and the route of product formation were analyzed.

Fig. 6 and 7 showed the SPD molecule analyzed by Gaussian 09. Fig. 6 showed that the C atoms (1C and 5C, 2C and 4C) on the ortho- and meta-positions of amino of benzene ring had strong electronegativity and the O atoms (15O and 16O) on the O=S=O functional group were easy to have electrophilic substitution reaction with the electrophilic oxidant NaOCl/OCl⁻.³⁴ Fig. 7 showed the electronegativity of 1C atom on benzene ring was the strongest (-0.247 v) and the electronegativity of 15O atom on O=S=O functional group was -0.767 v, which indicated that substitution reaction was more likely to occur in this site. It has also been reported that the H atom of amino position on aniline is easily replaced by Cl atom under chlorination and it has been proved in the chlorination reaction of microcystin³⁵ and phenacetin,³⁶ so the possibility of substitution reaction of 1C atom is the largest. The 19C and 20C atoms in pyridine ring were also prone to electrophilic substitution resulting in the breaking of 19C-20C bond. Therefore, the first step reaction was benzene ring substitution reaction and pyridine ring opening reaction. 4-Amino-*n*-methylbenzenesulfonamide, a ring opening product of pyridine with molecular weight (MW) of 186, was found by mass spectrometry. Moreover, according to the HOMO orbital analysis, the intermediate products with MW of 283 and MW of 268 can be predicted in the first step. The intermediate with molecular weight of 283 can form 4-amino-3-chloro-*n*-methylbenzenesulfonamide with molecular weight of 220 through ring opening of pyridine and then the amino group of 4-amino-3-chloro-*n*-methylbenzenesulfonamide was replaced by chlorine atom to form 3,4-dichlorobenzenesulfonic acid with molecular weight of 210. In addition, the amino group on SPD was replaced by Cl to form MW 268 intermediate and then the S-N bond in MW 268 intermediate product broke to form chlorobenzenesulfonic acid with MW 176. Chlorobenzenesulfonic acid formed 3,4-dichlorobenzenesulfonic acid through chlorine substitution reaction. According to the mass spectrum analysis and the prediction of HOMO and atomic charge distribution, the reaction pathway was proposed in Fig. 8.

4 Conclusion

In this study, the chlorinated degradation of SPD in both WDS and beakers was investigated. The degradation of SPD in WDS fits to both the first-order and pseudo second-order kinetic model. The change of pH has obvious influence on the reaction rate and the optimal pH condition for SPD degradation is around 7. A model then can be fitted through the ratio of the individual components to predict the first-order and pseudo second-order kinetic constants at different

pH values. The chlorination degradation rate of SPD increases obviously with the flow rate increasing. When the flow rate is above 1.0 m s⁻¹, the influence of the flow rate can be negligible. Due to the different iron ion concentration, the chlorination degradation capability of SPD is following: stainless-steel pipe > ductile iron pipe > PE pipe. Through comparison experiments, it is found that the total increase of THMs is 38.22 µg L⁻¹ at 6 h when the WDS contains SPD. The increase amount of THMs is only 8.85 µg L⁻¹ at 6 h without SPD, and the increase amount of THMs is almost zero at 6 h in the beakers. 4-Amino-*n*-methylbenzenesulfonamide, 4-amino-3-chloro-*n*-methylbenzenesulfonamide, 3,4-dichlorobenzenesulfonic acid and chlorobenzenesulfonic acid are four chlorination products of SPD based on LC-MS analysis. The DFT analysis revealed that the C atom on the ortho- and meta-positions of the amino group on the benzene ring. The O atom on the O=S=O functional group, and the 20C and 28 N atoms on the pyridine ring of the SPD molecule are strongly electronegative, which is easy react with the electrophilic oxidant NaOCl/OCl⁻.

Conflicts of interest

There are no conflicts to declare.

Acknowledgements

This work was supported by Natural Science Foundation of Shanghai (20ZR1438200) and National Natural Science Foundation of China (51778565).

References

- 1 H. Dong, X. Yuan, W. Wang and Z. Qiang, Occurrence and removal of antibiotics in ecological and conventional wastewater treatment processes: A field study, *J. Environ. Manage.*, 2016, **178**, 11-19.
- 2 T. Garoma, S. K. Umamaheshwar and A. Mumper, Removal of sulfadiazine, sulfamethizole, sulfamethoxazole, and sulfathiazole from aqueous solution by ozonation, *Chemosphere*, 2010, **79**, 814-820.
- 3 D. Cheng, H. H. Ngo, W. Guo, D. Lee, D. L. Nghiem, J. Zhang, S. Liang, S. Varjani and J. Wang, Performance of microbial fuel cell for treating swine wastewater containing sulfonamide antibiotics, *Bioresour. Technol.*, 2020, **311**, 123588.
- 4 H. Wang, W. Guo, R. Yin, J. Du, Q. Wu, H. Luo, B. Liu, F. Sseguya and N. Ren, Biochar-induced Fe(III) reduction for persulfate activation in sulfamethoxazole degradation: Insight into the electron transfer, radical oxidation and degradation pathways, *Chem. Eng. J.*, 2019, **362**, 561-569.
- 5 M. Conde-Cid, D. Fernandez-Calvino, M. J. Fernandez-Sanjurjo, A. Nunez-Delgado, E. Alvarez-Rodriguez and M. Arias-Estevez, Effects of pine bark amendment on the transport of sulfonamide antibiotics in soils, *Chemosphere*, 2020, **248**, 126041.

- 6 E. Y. Klein, T. P. Van Boeckel, E. M. Martinez, S. Pant, S. Gandra, S. A. Levin, H. Goossens and R. Laxminarayan, Global increase and geographic convergence in antibiotic consumption between 2000 and 2015, *Proc. Natl. Acad. Sci. U. S. A.*, 2018, **115**, E3463–E3470.
- 7 W. Baran, E. Adamek, J. Ziemianska and A. Sobczak, Effects of the presence of sulfonamides in the environment and their influence on human health, *J. Hazard. Mater.*, 2011, **196**, 1–15.
- 8 J. He, T. Xie, T. Luo, Q. Xu, F. Ye, J. An, J. Yang and J. Wang, Enhanced peroxymonosulfate activation over heterogeneous catalyst Cu_{0.76}Co_{2.24}O₄/SBA-15 for efficient degradation of sulfapyridine antibiotic, *Ecotoxicol. Environ. Saf.*, 2021, **216**, 112189.
- 9 J. Huang, A. R. Zimmerman, H. Chen and B. Gao, Ball milled biochar effectively removes sulfamethoxazole and sulfapyridine antibiotics from water and wastewater, *Environ. Pollut.*, 2020, **258**, 113809.
- 10 H. Zhang, X. Wei, X. Song, S. Shah, J. Chen, J. Liu, C. Hao and Z. Chen, Photophysical and photochemical insights into the photodegradation of sulfapyridine in water: A joint experimental and theoretical study, *Chemosphere*, 2018, **191**, 1021–1027.
- 11 J. Xu, Z. Hao, C. Guo, Y. Zhang, Y. He and W. Meng, Photodegradation of sulfapyridine under simulated sunlight irradiation: Kinetics, mechanism and toxicity evolution, *Chemosphere*, 2014, **99**, 186–191.
- 12 Y. Li, J. Chen, X. Qiao, H. Zhang, Y.-N. Zhang and C. Zhou, Insights into photolytic mechanism of sulfapyridine induced by triplet-excited dissolved organic matter, *Chemosphere*, 2016, **147**, 305–310.
- 13 F. Dong, C. Li, J. Crittenden, T. Zhang, Q. Lin, G. He, W. Zhang and J. Luo, Sulfadiazine destruction by chlorination in a pilot-scale water distribution system: Kinetics, pathway, and bacterial community structure, *J. Hazard. Mater.*, 2019, **366**, 88–97.
- 14 M. A. Mazhar, N. A. Khan, S. Ahmed, A. H. Khan, A. Hussain, Rahisuddin, F. Changani, M. Yousefi, S. Ahmadi and V. Vambol, Chlorination disinfection by-products in municipal drinking water – A review, *J. Cleaner Prod.*, 2020, **273**, 123159.
- 15 H. Liu, B. Zhang, Y. Li, Q. Fang, Z. Hou, S. Tian and J. Gu, Effect of Radical Species and Operating Parameters on the Degradation of Sulfapyridine Using a UV/Chlorine System, *Ind. Eng. Chem. Res.*, 2020, **59**, 1505–1516.
- 16 M. J. Rodriguez, J.-B. Sérodes and P. Levallois, Behavior of trihalomethanes and haloacetic acids in a drinking water distribution system, *Water Res.*, 2004, **38**, 4367–4382.
- 17 F. Dong, C. Li, X. Ma, Q. Lin, G. He and S. Chu, Degradation of estriol by chlorination in a pilot-scale water distribution system: Kinetics, pathway and DFT studies, *Chem. Eng. J.*, 2020, **383**, 123187.
- 18 F. Dong, C. Li, J. Crittenden, T. Zhang, Q. Lin, G. He, W. Zhang and J. Luo, Sulfadiazine destruction by chlorination in a pilot-scale water distribution system: Kinetics, pathway, and bacterial community structure, *J. Hazard. Mater.*, 2019, **366**, 88–97.
- 19 G. He, C. Li, F. Dong, T. Zhang, L. Chen, L. Cizmas and V. K. Sharma, Chloramines in a pilot-scale water distribution system: Transformation of 17 β -estradiol and formation of disinfection byproducts, *Water Res.*, 2016, **106**, 41–50.
- 20 F. Dong, Q. Lin, J. Deng, T. Zhang, C. Li and X. Zai, Impact of UV irradiation on *Chlorella* sp. damage and disinfection byproducts formation during subsequent chlorination of algal organic matter, *Sci. Total Environ.*, 2019, **671**, 519–527.
- 21 F. Zhu, J. Pan, Q. Zou, M. Wu, H. Wang and G. Xu, Electron beam irradiation of typical sulfonamide antibiotics in the aquatic environment: Kinetics, removal mechanisms, degradation products and toxicity assessment, *Chemosphere*, 2021, **274**, 129713.
- 22 K. Fukui, Role of Frontier Orbitals in Chemical Reactions, *Science*, 1982, **218**, 4574.
- 23 M. H. Yassine, A. Rifai, M. Hoteit, P. Mazellier and M. Al Iskandarani, Study of the degradation process of ofloxacin with free chlorine by using ESI-LCMSMS: Kinetic study, by-products formation pathways and fragmentation mechanisms, *Chemosphere*, 2017, **189**, 46–54.
- 24 W.-J. Shi, L.-X. Feng, X. Wang, Y. Huang, Y.-F. Wei, Y.-Y. Huang, H.-J. Ma, W. Wang, M. Xiang and L. Gao, A near-infrared-emission aza-BODIPY-based fluorescent probe for fast, selective, and “turn-on” detection of HClO/CLO⁻, *Talanta*, 2021, **233**, 122581.
- 25 H. Park, Y.-C. Hung and D. Chung, Effects of chlorine and pH on efficacy of electrolyzed water for inactivating *Escherichia coli* O157:H7 and *Listeria monocytogenes*, *Int. J. Food Microbiol.*, 2004, **91**, 13–18.
- 26 C. Ahmed Basha, P. A. Soloman, M. Velan, L. R. Miranda, N. Balasubramanian and R. Siva, Electrochemical degradation of specialty chemical industry effluent, *J. Hazard. Mater.*, 2010, **176**, 154–164.
- 27 N. Qi, H. Zhang, B. Jin and K. Zhang, CFD modelling of hydrodynamics and degradation kinetics in an annular slurry photocatalytic reactor for wastewater treatment, *Chem. Eng. J.*, 2011, **172**, 84–95.
- 28 M. Pérez-Moya, M. Graells, G. Castells, J. Amigó, E. Ortega, G. Buhigas, L. M. Pérez and H. D. Mansilla, Characterization of the degradation performance of the sulfamethazine antibiotic by photo-Fenton process, *Water Res.*, 2010, **44**, 2533–2540.
- 29 C.-W. Pai and G.-S. Wang, Treatment of PPCPs and disinfection by-product formation in drinking water through advanced oxidation processes: Comparison of UV, UV/Chlorine, and UV/H₂O₂, *Chemosphere*, 2022, **287**, 132171.
- 30 S. Li, X. Ao, C. Li, Z. Lu, W. Cao, F. Wu, S. Liu and W. Sun, Insight into PPCP degradation by UV/NH₂Cl and comparison with UV/NaClO: Kinetics, reaction mechanism, and DBP formation, *Water Res.*, 2020, **182**, 115967.
- 31 S. Ding, W. Chu, T. Bond, Q. Wang, N. Gao, B. Xu and E. Du, Formation and estimated toxicity of trihalomethanes, haloacetonitriles, and haloacetamides from the chlor(am)

- ination of acetaminophen, *J. Hazard. Mater.*, 2018, **341**, 112–119.
- 32 F. Dong, C. Li, G. He, X. Chen and X. Mao, Kinetics and degradation pathway of sulfamethazine chlorination in pilot-scale water distribution systems, *Chem. Eng. J.*, 2017, **321**, 521–532.
- 33 G. Velraj and S. Soundharam, Structure, vibrational, electronic, NBO and NMR analyses of 4-amino-N-[2-pyridinyl] benzene sulfonamide (sulfapyridine) by experimental and theoretical approach, *J. Mol. Struct.*, 2014, **1074**, 475–486.
- 34 M. Feng, X. Wang, J. Chen, R. Qu, Y. Sui, L. Cizmas, Z. Wang and V. K. Sharma, Degradation of fluoroquinolone antibiotics by ferrate(VI): Effects of water constituents and oxidized products, *Water Res.*, 2016, **103**, 48–57.
- 35 Y. Zhang, Y. Shao, N. Gao, W. Chu and Z. Sun, Removal of microcystin-LR by free chlorine: Identify of transformation products and disinfection by-products formation, *Chem. Eng. J.*, 2016, **287**, 189–195.
- 36 Y. Zhu, M. Wu, N. Gao, W. Chu, K. Li and S. Chen, Degradation of phenacetin by the UV/chlorine advanced oxidation process: Kinetics, pathways, and toxicity evaluation, *Chem. Eng. J.*, 2018, **335**, 520–529.

Appendix A. Supplementary data

Degradation of Sulfapyridine antibiotics by chlorination in a pilot-scale water distribution system: kinetics, THMs, and DFT studies

Jie Ji¹, Changjie Shi¹, Luo Xu¹, Kai Zhang¹, YunShu Zhang¹, Cong Li^{1,}, Eric*

Lichtfouse²

¹School of Environment and Architecture, University of Shanghai for Science and Technology,

Shanghai 200093, China

²Aix-Marseille Univ, CNRS, IRD, INRA, Coll France, CEREGE, 13100 Aix en Provence, France

E-mail: congil@aliyun.com

*Corresponding author.

Email addresses: congil@aliyun.com (C. Li)

Text S1 The introduction of pilot-scale WDS.

The WDS has three loops. Each loop is approximately 80 m in length and 150 mm in diameter. The pipe materials of three loops are ductile iron pipe, stainless steel and polyethylene plastic pipes (PE pipes). This system had the velocity controller and temperature controller. The flow rates could be adjusted from 0.2-1.8 m/s, and the temperature could be adjusted from 0 °C to 40 °C. In addition, this system was also equipped with an automatic detector, including free residual chlorine (FAC), turbidity, pH and so on. The ductile iron pipe was mostly used in this research, although stainless steel and PE pipes were tested. Experimental water circulated in the loop came from the municipal drinking water network in Hangzhou City.

Text S2 Dissociation reaction

(a) FAC

In aqueous solutions, due to dissociation reaction, residual chlorine generally has two forms of ClO^- and HClO as Equation (S1) .

$$[\text{FAC}] = [\text{HClO}] + [\text{ClO}^-] \quad (\text{S1})$$

Dissociation: $\text{HClO} \rightleftharpoons \text{ClO}^- + \text{H}^+$ $\text{pKa}=7.54$ Decomposition: $\text{HClO} \rightarrow \text{HCl} + \text{O}_2$ (S2)

Where, pKa is the dissociation constant of HClO , and there is $\text{pKa}=\lg\text{Ka}$. Then the Ka can be described as Equation (S3)

$$\text{Ka} = \frac{[\text{ClO}^-][\text{H}^+]}{[\text{HClO}]} \quad (\text{S3})$$

The proportions of HClO and ClO^- in aqueous solutions α_1 and α_2 can be determined as Equations (S4-S5).

$$\alpha_1 = \frac{[\text{H}^+]}{[\text{H}^+] + k_a^{\text{HClO}}} \quad (\text{S4})$$

$$\alpha_2 = \frac{k_a^{\text{HClO}}}{[\text{H}^+] + k_a^{\text{HClO}}} \quad (\text{S5})$$

Where $[\text{H}^+]$ can be determined by the pH of the reaction system.

(b) SPD

SPD also dissociates in aqueous solutions, and the dissociation is described as

Equations (S7-S8).

$$[SPD]_{tot} = [SPD^+] + [SPD] + [SPD^-]$$

$$SPD^+ = SPD + H^+ \quad pk_{a1}^{SPD} = 2.74 \quad (S7)$$

$$SPD = SPD^- + H^+ \quad pk_{a2}^{SPD} = 8.29 \quad (S8)$$

pk_{a1} and pk_{a2} are the first-order and second-order dissociation constants of SPD respectively and $pk_{a1} = pk_{a2}$, pk_{a1} and pk_{a2} are calculated as Equations (S9-S10).

$$k_{a1}^{SPD} = \frac{[SPD][H^+]}{[SPD^+]} \quad (S9)$$

$$k_{a2}^{SPD} = \frac{[SPD^-][H^+]}{[SPD]} \quad (S10)$$

Then the proportions of the three components of SPD can be described as Equations (S11-S13).

$$\beta_1 = \frac{[H^+]^2}{[H^+]^2 + [H^+]k_{a1}^{SPD} + k_{a1}^{SPD}k_{a2}^{SPD}} \quad (S11)$$

$$\beta_2 = \frac{[H^+]k_{a1}^{SPD}}{[H^+]^2 + [H^+]k_{a1}^{SPD} + k_{a1}^{SPD}k_{a2}^{SPD}} \quad (S12)$$

$$\beta_3 = \frac{k_{a1}^{SPD}k_{a2}^{SPD}}{[H^+]^2 + [H^+]k_{a1}^{SPD} + k_{a1}^{SPD}k_{a2}^{SPD}} \quad (S13)$$

The relationship between the total reaction and the orthogonal reaction of each component in the Equations (S14-S15).

$$\begin{aligned}
\frac{d[\text{SPD}]_{\text{tot}}}{dt} &= -k_2[\text{FAC}][\text{SPD}] = -\sum_{i=1}^2 \sum_{j=1}^3 k_{ij} \alpha_i [\text{FAC}] \beta_j [\text{SPD}] \\
&= -[\text{SPD}][\text{FAC}] \cdot \left\{ \begin{aligned}
&k_{11} \cdot \frac{[\text{H}^+]}{[\text{H}^+] + k_a^{\text{HOCl}}} \cdot \frac{[\text{H}^+]^2}{[\text{H}^+]^2 + [\text{H}^+] k_{a1}^{\text{SPD}} + k_{a1}^{\text{SPD}} k_{a2}^{\text{SPD}}} + \\
&k_{12} \cdot \frac{[\text{H}^+]}{[\text{H}^+] + k_a^{\text{HOCl}}} \cdot \frac{k_{a1}^{\text{SPD}} [\text{H}^+]}{[\text{H}^+]^2 + [\text{H}^+] k_{a1}^{\text{SPD}} + k_{a1}^{\text{SPD}} k_{a2}^{\text{SPD}}} + \\
&k_{13} \cdot \frac{[\text{H}^+]}{[\text{H}^+] + k_a^{\text{HOCl}}} \cdot \frac{k_{a1}^{\text{SPD}} \cdot k_{a2}^{\text{SPD}}}{[\text{H}^+]^2 + [\text{H}^+] k_{a1}^{\text{SPD}} + k_{a1}^{\text{SPD}} k_{a2}^{\text{SPD}}} + \\
&k_{21} \cdot \frac{k_a^{\text{HOCl}}}{[\text{H}^+] + k_a^{\text{HOCl}}} \cdot \frac{[\text{H}^+]^2}{[\text{H}^+]^2 + [\text{H}^+] k_{a1}^{\text{SPD}} + k_{a1}^{\text{SPD}} k_{a2}^{\text{SPD}}} + \\
&k_{22} \cdot \frac{k_a^{\text{HOCl}}}{[\text{H}^+] + k_a^{\text{HOCl}}} \cdot \frac{k_{a1}^{\text{SPD}} [\text{H}^+]}{[\text{H}^+]^2 + [\text{H}^+] k_{a1}^{\text{SPD}} + k_{a1}^{\text{SPD}} k_{a2}^{\text{SPD}}} + \\
&k_{23} \cdot \frac{k_a^{\text{HOCl}}}{[\text{H}^+] + k_a^{\text{HOCl}}} \cdot \frac{k_{a1}^{\text{SPD}} \cdot k_{a2}^{\text{SPD}}}{[\text{H}^+]^2 + [\text{H}^+] k_{a1}^{\text{SPD}} + k_{a1}^{\text{SPD}} k_{a2}^{\text{SPD}}}
\end{aligned} \right\} + \text{b} \tag{S14}
\end{aligned}$$

$$\begin{aligned}
k_2 = & \left\{ \begin{aligned}
&k_{11} \cdot \frac{[\text{H}^+]}{[\text{H}^+] + k_a^{\text{HOCl}}} \cdot \frac{[\text{H}^+]^2}{[\text{H}^+]^2 + [\text{H}^+] k_{a1}^{\text{SPD}} + k_{a1}^{\text{SPD}} k_{a2}^{\text{SPD}}} + \\
&k_{12} \cdot \frac{[\text{H}^+]}{[\text{H}^+] + k_a^{\text{HOCl}}} \cdot \frac{k_{a1}^{\text{SPD}} [\text{H}^+]}{[\text{H}^+]^2 + [\text{H}^+] k_{a1}^{\text{SPD}} + k_{a1}^{\text{SPD}} k_{a2}^{\text{SPD}}} + \\
&k_{13} \cdot \frac{[\text{H}^+]}{[\text{H}^+] + k_a^{\text{HOCl}}} \cdot \frac{k_{a1}^{\text{SPD}} \cdot k_{a2}^{\text{SPD}}}{[\text{H}^+]^2 + [\text{H}^+] k_{a1}^{\text{SPD}} + k_{a1}^{\text{SPD}} k_{a2}^{\text{SPD}}} + \\
&k_{21} \cdot \frac{k_a^{\text{HOCl}}}{[\text{H}^+] + k_a^{\text{HOCl}}} \cdot \frac{[\text{H}^+]^2}{[\text{H}^+]^2 + [\text{H}^+] k_{a1}^{\text{SPD}} + k_{a1}^{\text{SPD}} k_{a2}^{\text{SPD}}} + \\
&k_{22} \cdot \frac{k_a^{\text{HOCl}}}{[\text{H}^+] + k_a^{\text{HOCl}}} \cdot \frac{k_{a1}^{\text{SPD}} [\text{H}^+]}{[\text{H}^+]^2 + [\text{H}^+] k_{a1}^{\text{SPD}} + k_{a1}^{\text{SPD}} k_{a2}^{\text{SPD}}} + \\
&k_{23} \cdot \frac{k_a^{\text{HOCl}}}{[\text{H}^+] + k_a^{\text{HOCl}}} \cdot \frac{k_{a1}^{\text{SPD}} \cdot k_{a2}^{\text{SPD}}}{[\text{H}^+]^2 + [\text{H}^+] k_{a1}^{\text{SPD}} + k_{a1}^{\text{SPD}} k_{a2}^{\text{SPD}}}
\end{aligned} \right\} + \text{b} \tag{S15}
\end{aligned}$$

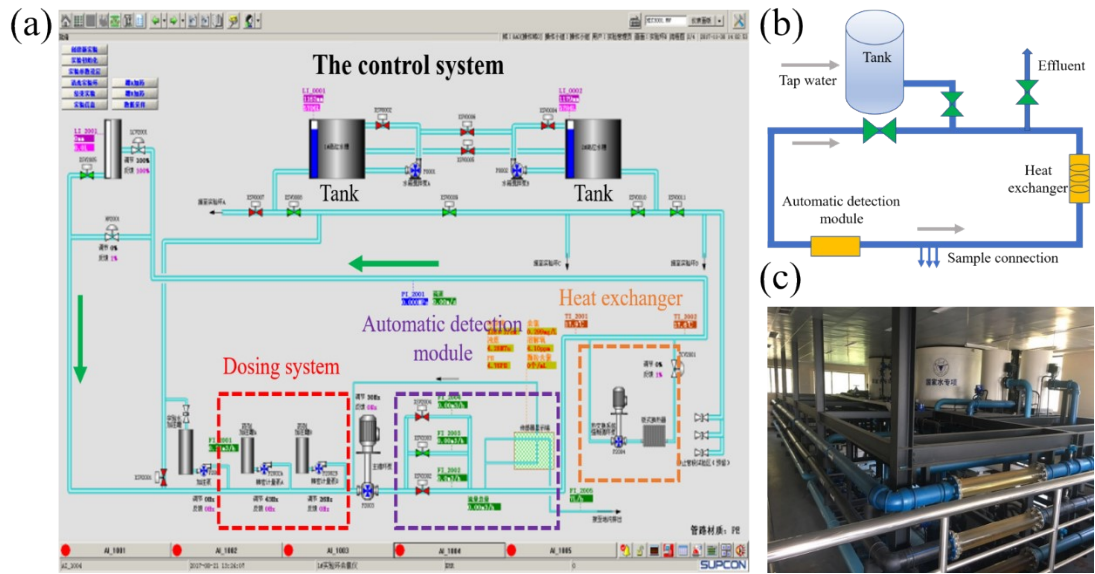


Fig. S1 Schematic representation of WDS. (a): The control system for the WDS. (b): The illustration of WDS model. (c): The pilot-scale WDS in experiments.

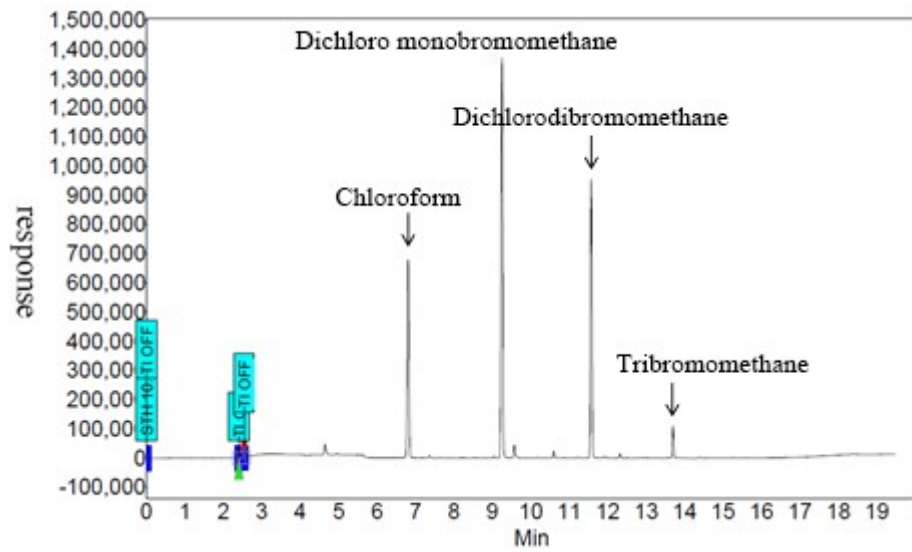


Fig. S2 GC-ECD chromatogram of trihalomethane.

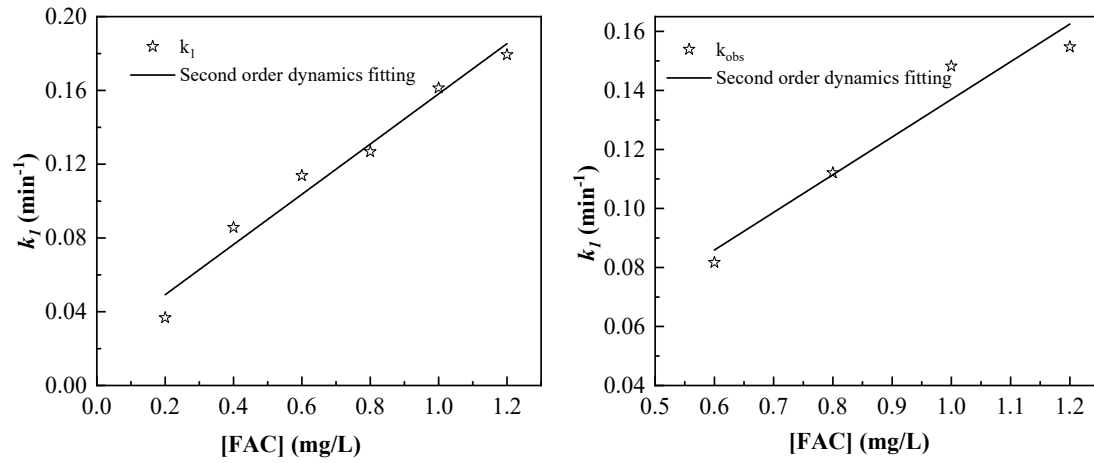


Fig. S3 (a) Second order dynamic fitting in WDS; (b) Second order dynamics fitting in beaker tests;

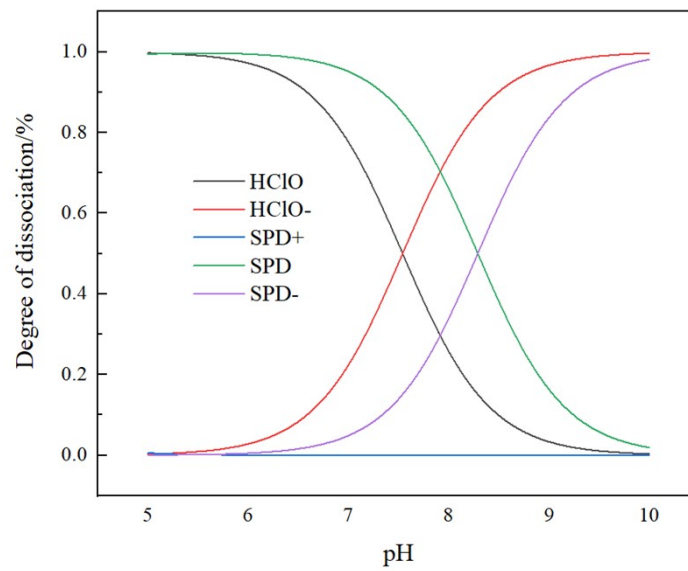


Fig.S4 Distribution coefficient of each component at different pH

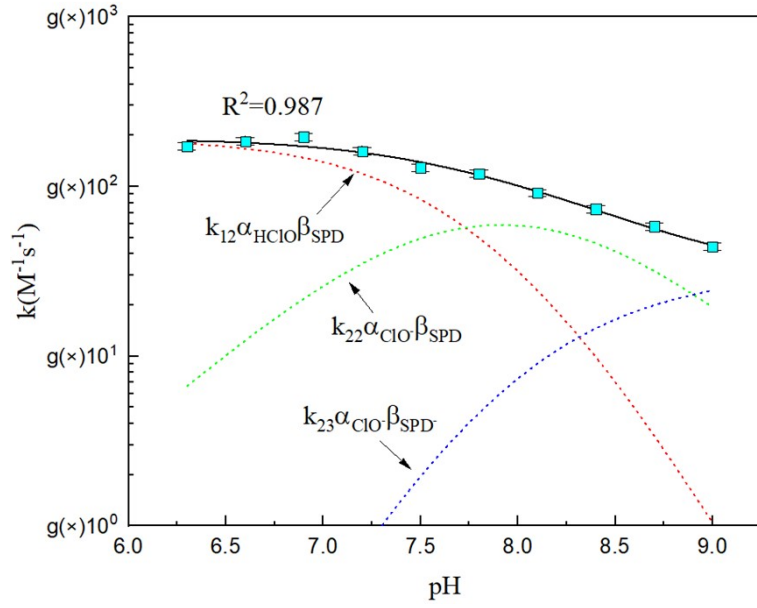
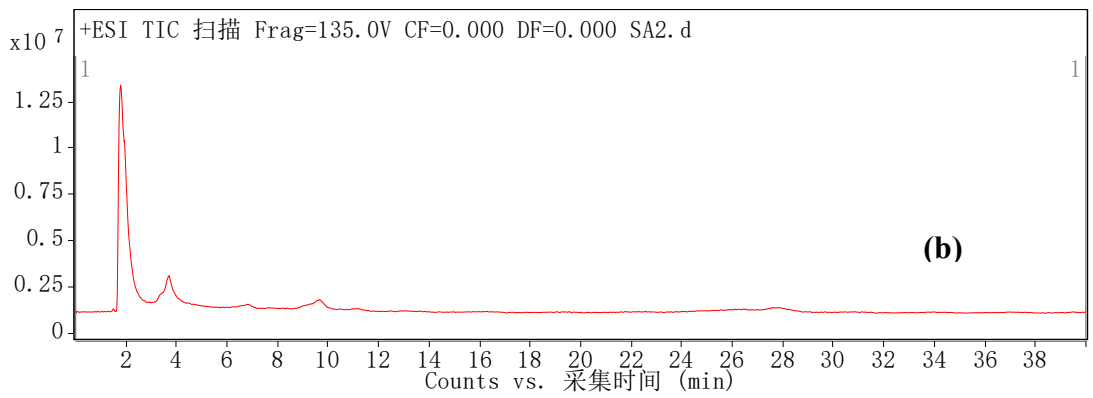
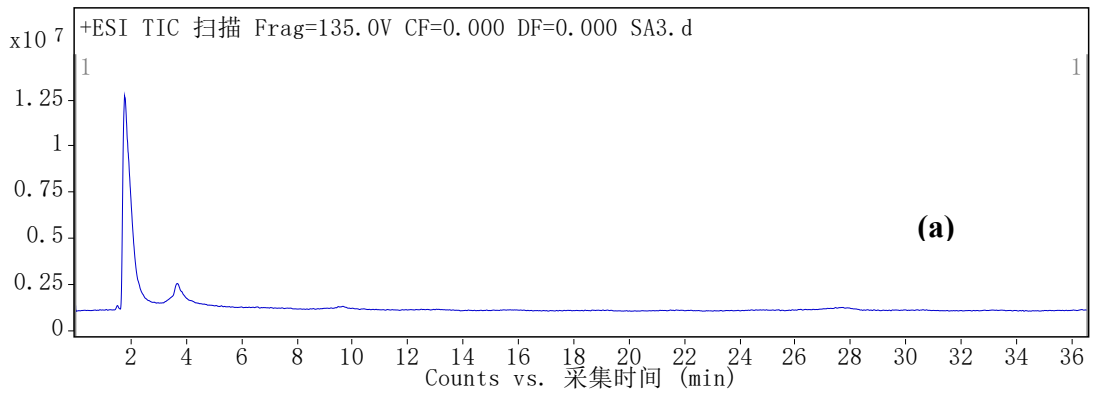


Fig. S5 k_2 and pH model of SPD chloride in WDS and beaker tests.



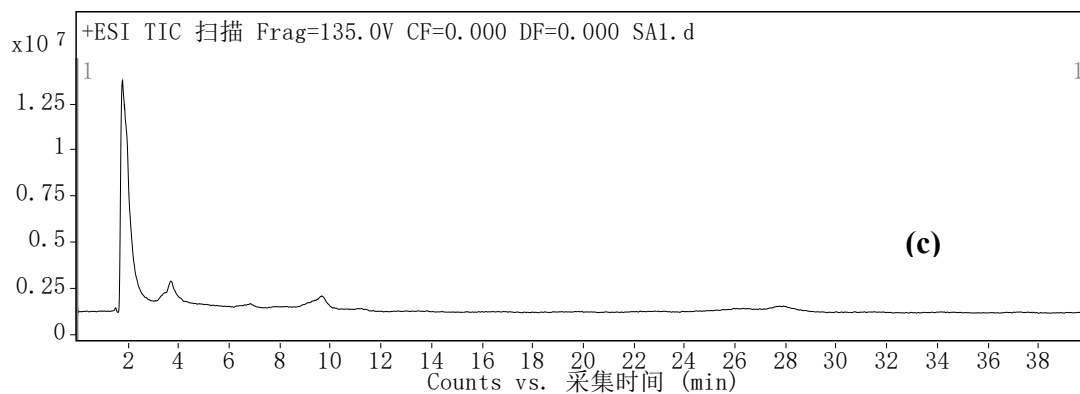
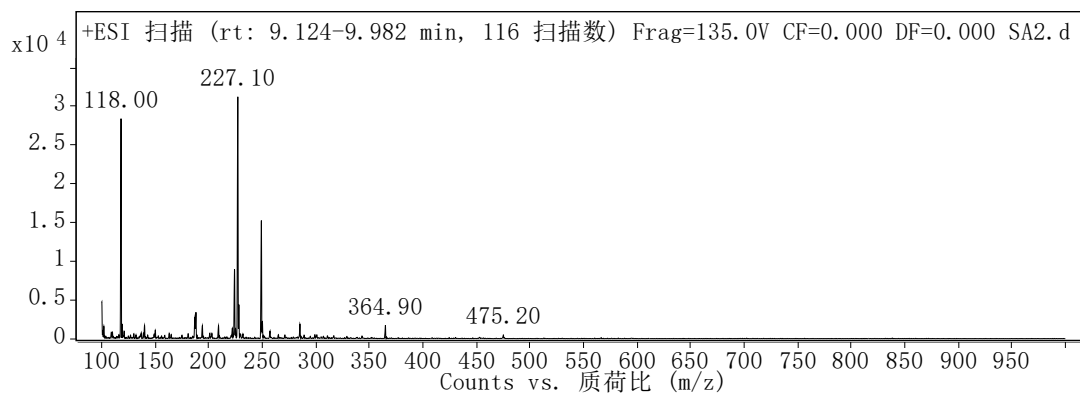
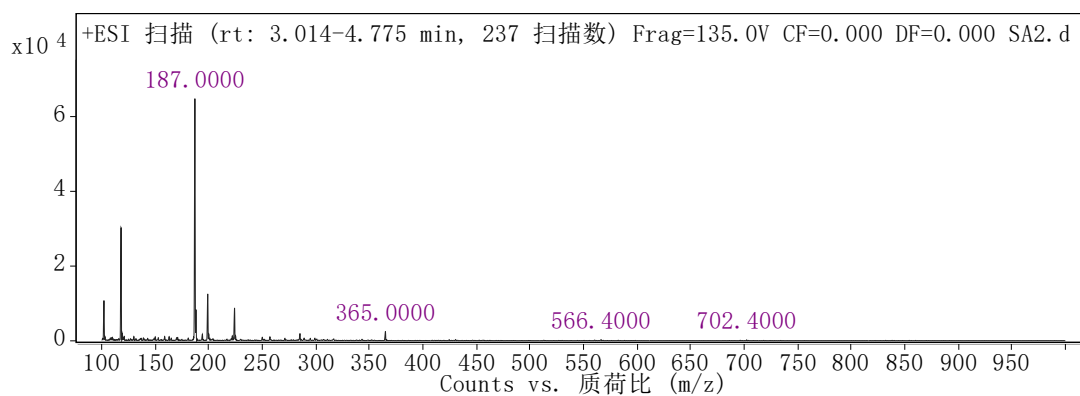
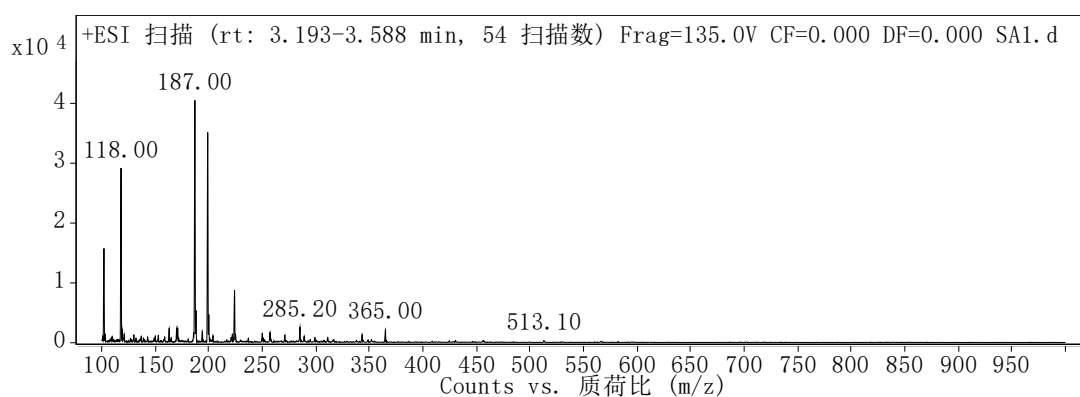


Fig S6 LC-MS scans in positive ion mode (ESI+): (a) (b) (c) 10 min, 20 min and 30 min reaction samples, respectively



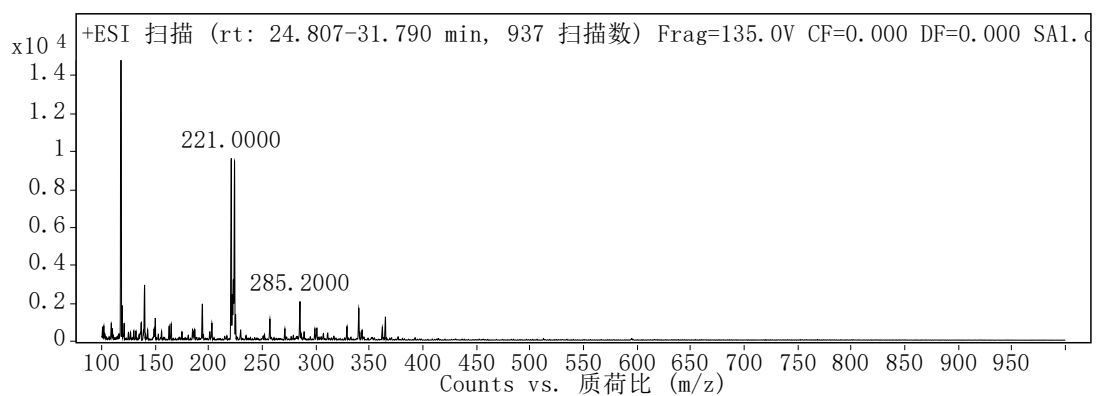


Fig. S7 Mass spectrum with different retention times. (a) 3.19-3.59 min, m/z 199; (b) 3.59-4.78 min, m/z 187 (c) 9.12-9.98 min, m/z 249 (d) 24.80-31.80 min, m/z 221

Table S1 Physiochemical characteristics of SPD

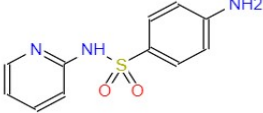
Chemical structure	Molecular formula	Boiling point	Melting point	Solubility in water
	C ₁₀ H ₁₀ N ₄ O ₂ S	473.5±51.0 °C	191-193°C	<0.1 g/100 mL at 22 °C

Table. S2 Parameter of injection system for purge and trap pretreatment.

Parameter name	Parameter value	Parameter name	Parameter value
Purge temperature	30	Analytical temperature	210
Purge time	15	Analysis time	3
Purge air flow	40	Baking temperature	250
Dry purge time	1.5	baking time	5
Dry purge flow	100	Injection volume of water sample	30

Table. S3 THMs standard curve.

Target analyte	Peak time	linear equation	R ²	Linear range	detection limit
Chloroform	6.90	Y=2067.2x+1542.3	0.9964	0~20	0.01
Dichloromethane	9.23	Y=20145x+1638	0.9985	0~20	0.01
Chlorodibromomethane	11.52	Y=21023x-1569.7	0.9923	0~20	0.01
Tribromomethane	13.72	Y=6457.3x+364.1	0.9945	0~20	0.01

Table. S4 The first order kinetic constant of the chlorination SPD reaction

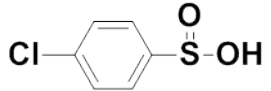
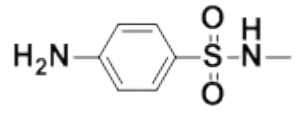
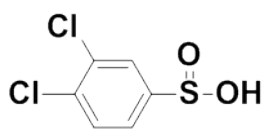
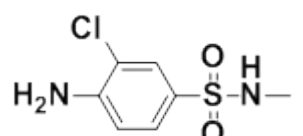
Residual chlorine concentration	k_l (min ⁻¹)		R^2	
	WDS	Beaker tests	WDS	Beaker tests

(mg/L)				
0.2	/	$(3.68 \pm 0.24) \times 10^{-2}$		0.967
0.4	/	$(8.51 \pm 0.16) \times 10^{-2}$		0.967
0.6	$(8.07 \pm 0.22) \times 10^{-2}$	$(11.35 \pm 0.18) \times 10^{-2}$	0.994	0.998
0.8	$(11.14 \pm 0.61) \times 10^{-2}$	$(12.65 \pm 0.26) \times 10^{-2}$	0.985	0.998
1.0	$(14.74 \pm 0.98) \times 10^{-2}$	$(16.13 \pm 0.40) \times 10^{-2}$	0.978	0.997
1.2	$(15.46 \pm 1.25) \times 10^{-2}$	$(17.98 \pm 0.57) \times 10^{-2}$	0.962	0.995

Table. S5 The second order kinetic constants of chlorination SPD reaction (k_2)

condition	WDS	Beaker tests
k_2 ($L \cdot mg^{-1} \cdot min^{-1}$)	$(12.89 \pm 2.22) \times 10^{-2}$	$(13.67 \pm 1.18) \times 10^{-2}$

Table S6 Molecular structures corresponding to different ionic fragment mass-to-charge ratios.

Retention time	(m/z)	Possible molecular formula	molecular weight
3.3 min	199		176
4.3 min	187		186
9.5 min	249		210
27.6 min	221		220